# Wave propagation in one-dimensional microscopic granular chains

Wei-Hsun Lin[1,2] and Chiara Daraio[2,3]
[1]*Department of Physics, California Institute of Technology, Pasadena, California 91125, USA*
[2]*Mechanical and Process Engineering, ETH Zurich, 8092 Zurich, Switzerland*
[3]*Engineering and Applied Science, California Institute of Technology, Pasadena, California 91125, USA*
(Received 7 July 2016; revised manuscript received 4 October 2016; published 28 November 2016)

We employ noncontact optical techniques to generate and measure stress waves in uncompressed, one-dimensional microscopic granular chains, and support our experiments with discrete numerical simulations. We show that the wave propagation through dry particles (150 $\mu$m radius) is highly nonlinear and it is significantly influenced by the presence of defects (e.g., surface roughness, interparticle gaps, and misalignment). We derive an analytical relation between the group velocity and gap size, and define bounds for the formation of highly nonlinear solitary waves as a function of gap size and axial misalignment.

DOI: 10.1103/PhysRevE.94.052907

## I. INTRODUCTION

Ordered granular systems, often referred to as granular crystals, are discrete arrays of solid particles arranged in periodic lattice geometries. Macroscopic granular crystals, composed of particles in the centimeter scale, have been a subject of active research [1–6]. Granular crystals have been shown to mediate nonlinear wave phenomena such as solitary waves [1] and intrinsic localized modes [7], which are of fundamental scientific interest. The dynamic response of granular crystals is governed by highly nonlinear interactions between neighboring particles, which is determined by their contact geometry (e.g., Hertzian). More generally, by modifying the contact geometry and particle arrangements (i.e., changing the stress-strain relation and the direction of contact forces) [8], granular crystals can be designed to behave as highly flexible waveguides [9], focusing lenses [10], and filtering materials [11]. These features of granular crystals have inspired their use in engineering applications, such as shock mitigation [12–15], acoustic rectification [16], and logic elements [17]. However, the macroscopic size of the particles tested experimentally to date imposes important limitations to their applicability. The particle diameters determine the length scale of the stress wave that can be transmitted through the granular assemblies. For example, applications in acoustic medical imaging or nondestructive evaluation, which employ acoustic pulses in the ultrasonic range, require particle sizes in the order of micrometers. Recent numerical work investigated the stress propagation in nanometer-scale particle chains composed of buckyballs, detailing important dynamic effects rising at ultrasmall scales [18]. However, not much is known to date about the response of granular chains in the micrometer range.

In this work we study the stress wave propagation in dry, one-dimensional microscopic granular chains using experiments and numerical simulations. Despite the fundamental importance of understanding the dynamics of microparticle assemblies, very little experimental work to date has been conducted at these scales. The lack of experimental investigation results from two major difficulties: (i) the absence of reliable methods to assemble and characterize dry microparticles in controlled configurations, and (ii) the need for a systematic way to excite microscopic granular particles without influencing the response of the system. Experimental techniques employed for macroscopic granular systems include manually assembled chains of particles, piezotransducers for applying excitation [19], and sensors embedded in particles for force measurements [20]. At the microscale, these techniques are not applicable. The nonlinear interactions in granular systems [21] are sensitive to the particle packing geometry and initial conditions. To ensure uniform contacts between microparticles, a high accuracy in particle positioning is necessary. In addition, the application of controlled excitations and the measurement of the propagating stresses cannot be achieved using contact methods, which are not sufficiently accurate and intrusive.

To overcome these experimental challenges, we constructed an experimental apparatus [Fig. 1(a)], which employs a computer-controlled micromanipulation system for the chain assembly, and noncontact optical techniques for the characterization [21], as described in the next section.

## II. EXPERIMENTAL SETUP AND THEORETICAL MODELING

In this work, we study microscopic granular chains composed of stainless steel particles (type 316 and 440c) with radii of 150 $\mu$m. The steel 316 particles have a nominal surface roughness and radius variation of $\sim$3 $\mu$m, while the steel 440c particles have a roughness of 0.1 $\mu$m and a radius variation of $\sim$1 $\mu$m, as provided by the manufacturer specifications (New England Miniature Ball). The chains of particles are assembled on supporting microgrooves, and aligned with a micromanipulator, to ensure packing repeatability. The microgrooves have a v-shaped cross section, which confines the motion of the microparticles in one dimension. The grooves are fabricated on silicon wafers by chemical etching with potassium hydroxide and have opening widths of 240 $\mu$m [Fig. 1(c)]. To assemble the microparticles in one-dimensional chains, the particles are first randomly deposited into the grooves, and then compressed from both ends and positioned adjacent to each other with the micromanipulator (Zaber LSM025). The micromanipulator tip, controlled by a stepper motor with a precision of 0.05 $\mu$m, is retracted after assembling the chains, leaving the chains with free boundaries. The

 

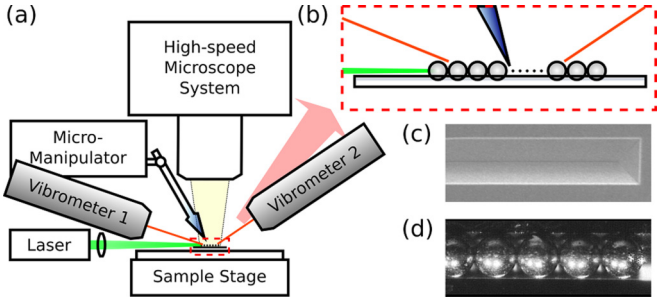


FIG. 1. Schematic diagram of the experimental setup. (a) The system consists of a laser excitation system, a high-speed microscopy imaging system, two vibrometers, and a micromanipulator. (b) The incoming focused laser beam (15-$\mu$m beam waist) is used to excite stress waves in the chains. The imaging system is used to record the particle motion in high speed, and the vibrometers are used to measure the velocity profiles of selected microparticles. (c) Scanning electron microscopy image of the v-shaped groove supporting the chain (the angle between two inclined planes is 70.6°). (d) Optical microscope image of a microscopic granular chain assembled on the supporting structure.

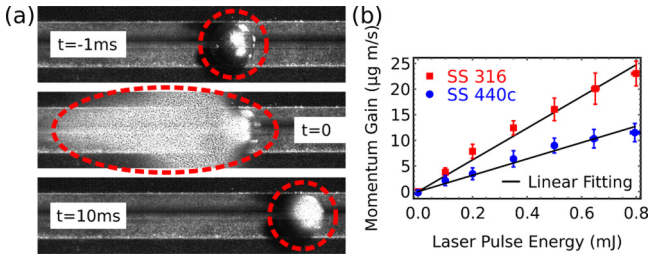


FIG. 2. Excitation of microparticles via pulsed laser ablation. (a) The high-speed images of a particle before and after being illuminated by a pulsed laser. The light pattern on the particle changes after excitation due to laser-induced surface damages. (b) The observed momentum gains of stainless steel type 316 (red square) and 440c (blue circle) particle at varying pulse energy. The error bars represent 1 standard deviation for each data point derived from 20 experimental runs.

resulting granular chains are not precompressed. In macroscopic granular systems, the application of a static, external precompressive force is commonly used to compact the chains and tune their dynamic response [22]. In microscopic chains, the application of a controlled, static compressive force is more difficult and the use of fixed boundary conditions (e.g., a wall at the end of the chain) can interfere with the initial excitation. In this work, we focus on the study of uncompressed microgranular chains with free boundaries.

During assembly, the chains [Fig. 1(d)] are inspected with a high-speed microscopy imaging system (Vision Research Phantom v12.1, Leica S6D) which can track their position with a 2-$\mu$m precision at 25 kHz. To reduce the effects of the particle polydispersity, we assemble each chain multiple times and measure the overall chain lengths. We select for testing only the chains with shorter and equal lengths. The maximum number of microparticles that can be included in a chain is limited experimentally by the need for optical inspection of the assemblies and the micromanipulator tip. The field of view of our imaging system is ~6 mm and allows for simultaneously visualizing the assembly of chains with a maximum of 20 particles. We select for testing chains composed of 15 particles. Macroscopic chains of similar lengths have been shown to support the formation and propagation of nonlinear solitary waves [1,2,4]. Also, numerical simulations (described below) of propagating stress waves in an ideal 15-particle chain showed that the pulse amplitude at the end of the chain differs by $<1\%$ from pulses in an infinite chain [2].

The selected microparticle chains are excited by a striker particle (particle 1 in our assembly), identical to the others, set in motion by a Q-switched pulsed laser (Quantel Brilliant, 532 nm, 4 ns). The intense laser pulse induces vaporization and ejection of material from the surface of the illuminated particle [Fig. 2(a)], transferring an initial momentum [23]. The pulse laser energy intensity, the pulse duration, and the thermal properties of the particle's material all affect the momentum transfer [23]. We characterize the relation between pulse energy and the momentum gain for our specific experimental configuration, targeting individual particles initially resting on the v-shaped groove and monitoring the resulting particle trajectories. We vary the pulse energy of the laser beams from 0 to 0.8 mJ and test the momentum gained by particles made of both stainless steel type 316 and 440c [Fig. 2(b)]. While these two materials have similar elastic properties, such as Young's modulus and Poisson's ratio, they have distinct thermal properties (for example, specific heat and thermal conductivity for stainless steel type 316 at 100 °C are 0.50 kJ kg K and 16.2 W m K, and 0.46 kJ kg K and 24.2 W m K for type 440c) [24], which lead to a significantly different response to laser ablation [Fig. 2(b)]. Both types of particles show a linear momentum gain within the range of the tested pulse energy but with different gain-to-energy ratios. We use this characterization to estimate the initial velocity of the striker particles later used in the experiments with granular chains.

We test microscopic granular chains at varying initial striker velocity ($v_s$), from 0.005 to 0.1 m s, and measure the stress wave propagation. To measure the wave propagation through the chains, we employ two laser vibrometers (Polytec OFV-534), which monitor the velocity profiles of the 2nd and 13th particles. Because of the angles between the axis of the chains and the beams of the vibrometers, the output of the vibrometers includes off-axis components (with respect to the chains axis). To ensure the correct detection of the on-axis velocities, we perform an independent calibration of both vibrometers. For the calibration, we focus the vibrometers on the targeted particles in the assembled chain and shift the computer-controlled sample stage with known on-axis velocities. The vibrometer output is monitored and compared with the stage velocity to obtain a calibration factor.

We use numerical simulations to inform our experiments. We model the granular chains with a discrete element model using Hertzian contact interactions and simulate the evolution of the system with a fourth-order Runge-Kutta solver. The contact force $f_c$ between two neighboring particles is

$$f_c = \frac{2}{3}\frac{E}{1-\nu^2}\sqrt{\frac{R}{2}}(2R - |x_m - x_n|)_+^{3/2}, \quad (1)$$

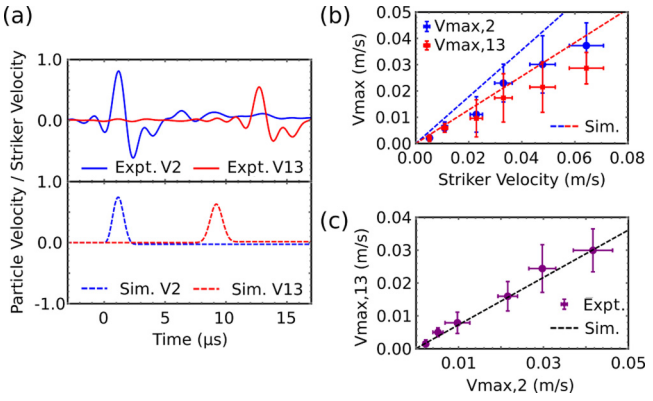


FIG. 3. Measured particle velocity profile in a microscopic granular chain of 15 stainless steel 440c particles with laser excitation. (a) Experimental measurement (solid lines) and numerical prediction (dashed lines) of velocities of the 2nd (blue) and 13th (red) particles in the chain (normalized to the striker velocities). (b) Measured maximum velocities at varying striker velocities compared with the corresponding numerical prediction (dashed lines). Error bars represent 1 standard deviation. (c) Ratio between maximum velocities of the two monitored particles at varying striker velocities. The corresponding numerical prediction is plotted with a dashed line. Error bars represent 1 standard deviation.

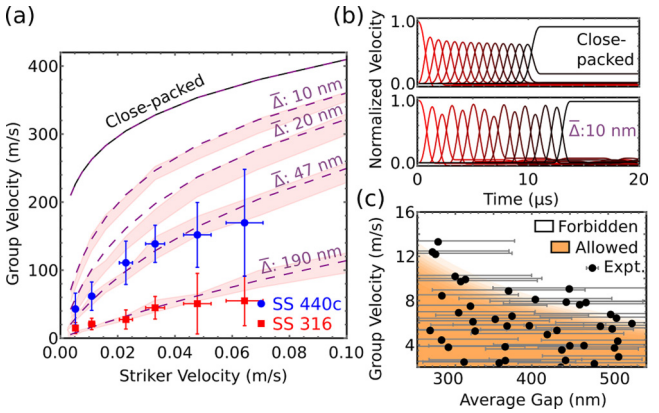


FIG. 4. (a) Group velocities of a signal traveling in uncompressed microscopic granular chains. Experimental data for the two types of stainless steel particles are shown as solid dots and squares with error bars (1 standard deviation). The shaded bands represent the group velocities of random samples of uncompressed chains with average interparticle gap sizes of 0 (close-packed), 10, 20, 47, and 190 nm. The dashed lines are the corresponding prediction obtained with Eq. (2). (b) Comparison of particle velocities (normalized to the striker velocity) in a close-packed microscopic granular chain and in a randomly generated chain with an average gap of 10 nm. The chains consist of 15 stainless steel particles (440c) with a radius of 150 $\mu$m, excited by an initial striker velocity of 0.1 m s. (c) Distribution of group velocity at different average interparticle gaps based on 45 measurements and their corresponding experimental uncertainty. The orange and white area represents the "allowed" and "forbidden" zone for the measured group velocity defined by the analytical upper bound from Eq. (2). The boundary between the allowed and forbidden zones is illustrated with gradient color between orange and white due to the uncertainty in estimation of the striker velocity in Eq. (2).

where $x_m$ and $x_n$ are the coordinates of the two particles, $R$ is the radius, $E$ the elastic modulus, and $\nu$ the Poisson ratio of the particles. The subscript to the bracket notation, defined by $(x)_+ \equiv \max(x,0)$, indicates the tensionless behavior of the system. All parameters used in the model are derived from experimental data and we neglect dissipation.

## III. MAIN RESULTS

A typical velocity profile measurement is shown in Fig. 3(a) for a wave excited by a striker with velocity 0.1 m s. The blue and red solid lines correspond to the velocity profile measured for particles 2 and 13, respectively. The corresponding numerical results are plotted for comparison in the lower panel with dashed lines. The difference in the pulse shape observed between the experiments and the numerical simulations can be partially attributed to the limited bandwidth of the laser vibrometers available for testing (2.5 MHz). The vibrometer's limited bandwidth acts as a filter to the recorded signal. Reconstruction of the original wave form profile requires a detailed calibration of the frequency and phase response of the vibrometer outside of its typical working frequency in the particular experimental configuration selected. Due to difficulties in obtaining such reconstruction, we focus our discussions on the particle and group velocities of the propagating waves (which are not affected by the vibrometers' bandwidth). We define $v_{\max,2}$ and $v_{\max,13}$ as the maximum particle velocities of the 2nd and 13th particles, respectively, and compare them with the numerical results $v_{\max,2}{}^{(\mathrm{sim})}$ and $v_{\max,13}{}^{(\mathrm{sim})}$. In Fig. 3(b), we plot the measured $v_{\max,2}$ and $v_{\max,13}$ at different striker velocities $v_s$, together with the corresponding prediction from simulation (dashed lines). We obtain the average values of $v_{\max,2} = (0.57 \pm 0.09)v_s$ and $v_{\max,13} = (0.46 \pm 0.07)v_s$ (with a 95% confidence interval in a linear fitting model), which is 40% smaller compared to the numerical prediction, $v_{\max,2}{}^{(\mathrm{sim})} = 0.89v_s$ and $v_{\max,13}{}^{(\mathrm{sim})} = 0.64v_s$. However, their ratio $v_{\max,13}/v_{\max,2} = 0.80 \pm 0.08$ agrees well with the corresponding numerical prediction, $v_{\max,13}{}^{(\mathrm{sim})}/v_{\max,2}{}^{(\mathrm{sim})} = 0.72$, shown in Fig. 3(c). This suggests that the deviation of the measured $v_{\max,2}$ and $v_{\max,13}$ from numerical data is a result of the wave form deformation due to the limited measurement bandwidth, in addition to the presence of dissipation in experiments.

Although the measured relative particle velocity agrees well with numerical simulations, the wave's group velocity is significantly lower in experiments than in numerical simulations. We plot the measured group velocity $v_g{}^{(\mathrm{meas})}$ as a function of the striker velocity [Fig. 4(a)]. Here, $v_g{}^{(\mathrm{meas})} = (13-2)2R/\Delta t$, where $\Delta t$ is the time delay between the maximum amplitudes of $v_2$ and $v_{13}$. For both types of stainless steel particles tested, the measured group velocity (solid symbols with error bar) varies nonlinearly with the striker velocity, which is a clear indication that the wave propagation within the granular assemblies is governed by nonlinear interactions. However, the measured group velocities are significantly lower than the numerical prediction for close-packed microscopic granular chains [solid line in Fig. 4(a)]. In addition, the stainless steel 440c particles have higher group velocities than stainless steel 316, despite that the two types of stainless steel have similar elastic properties.

In order to explain this deviation between measurement and numerical simulations, we study the role of defects and packing imperfection in the wave propagation. We focus on the presence of interparticle gaps, which are expected to be in the order of magnitude of the particles' surface roughness ($\ll R$), and as such below optical resolution of our experimental characterization system. We model the dynamics of one-dimensional chains with interparticle gaps varying between 0 and 200 nm and investigate how the gaps affect the group velocity of the propagating wave. We generate random initial configurations of 15 particles with average gap sizes ($\bar{\Delta}$) per particle of 10, 20, 47, and 190 nm, and calculate the group velocities for different striker velocities. For each gap size and striker velocity, we simulate 100 configurations and plot the distribution of the resulting group velocities [shaded bands in Fig. 4(a)]. As the average gap sizes increase, the calculated group velocity deviates more from the group velocity expected in a perfectly packed system. The differences in the measured group velocities between the stainless steel 316 and 440c microparticle chains could therefore be explained by assuming bigger, more effective interparticle gaps between the 316 particles. This can be related to the difference in surface roughness and size variation of the two materials, reportedly higher in the 316 particles. While our sample preparation procedures include micromanipulator compression and visual inspection of the chain, an ideal close-packing condition cannot be guaranteed. We thus expect larger interparticle gaps in chains of free, noncompressed particles with higher polydispersity. However, the average gap sizes suggested by the numerical fitting [in Fig. 4(a)] are smaller than the polydispersity for the 316 and 440c particles. This can be partially explained by considering three-dimensional effects in the particles' positioning within the support grooves. Variations in the radii (arising from the particles' polydispersity) result in a vertical misalignment of the particle centers from the main chain's axis. This misalignment reduces the effective center-to-center distance between the particles and results in smaller gaps in the one-dimensional model used in our analysis.

Accounting for the presence of average gaps in the chains, the deviation of the group velocity from the close-packed configuration can be explained by the following relation:

$$\frac{2R+\bar{\Delta}}{v_g{}^{(\mathrm{meas})}} \approx \frac{2R}{v_g{}^{(0)}} + \frac{\bar{\Delta}}{v_s}, \tag{2}$$

where $v_g{}^{(0)}$ is the group velocity of the solitary wave propagating in an ideal, uncompressed close-packed granular chain. Equation (2) assumes that the measured time of flight for the pulse is the sum of the traveling time of a solitary wave propagating in a close-packed granular chain and the traveling time of the individual particles to close the gap to reach the next particle. We plot the values predicted by Eq. (2) with dashed lines in Fig. 4(a), which lies above the distribution of group velocities obtained in simulation of chains with corresponding average gaps. The particle velocity can lie between two bounds: (i) For an ideal chain excited by a striker particle which has the same mass as other particles in the chain, the maximum particle velocity is $v_{\max} = \frac{25}{16}(\frac{v_g{}^{(0)}}{c})^4 v_g{}^{(0)}$, where $c = \sqrt{\frac{2}{\pi}\frac{E}{\rho(1-\nu^2)}}$ is the sound speed in the material of the particle [1] and $\rho$ is the density. (ii) For a chain with all particles separated from each other, in the absence of losses, momentum conservation imposes that each particle velocity is equal to the striker velocity. Equation (2) defines the relation between the group velocity and the presence of interparticle gaps when chains in an experimental system lie between these two bounds. By fitting Eq. (2) with different average gap sizes, we can explain the reduction of group velocity in the different steel chains tested experimentally. For example, the measured group velocity for a chain composed of stainless steel 316 particles, with a rougher surface finish, agrees well with the numerical model if we assume an average, effective, average interparticle gap of 190.4 nm. Similarly, the effective, average gaps for the chain of 440c steel particles (with a smoother surface) is estimated to be 47 nm. Note that relatively small gaps (in our case, $\sim 0.03\%-0.1\%$ of the radii of the particles) can have a significant impact on the measured group velocities. This results from the fact that the striker velocity is about 4 orders of magnitude smaller than the group velocity in an ideal chain.

To gain more insight on the influence of interparticle gaps in the dynamics of these systems, we compare the wave propagation properties in an ideal chain composed of 15 particles with the response of the chain with only 10-nm average interparticle gaps. We perform numerical simulations and plot the velocity profiles of the 15 particles in Fig. 4(b). The particle velocities in an ideal, close-packed chain follow the profile expected from the formation of a highly nonlinear solitary wave [1]. However, the particle velocity profile calculated for the chain with a randomly distributed interparticle gaps shows irregular oscillation as the wave propagates along the chain (and their value is larger than the ideal case). We study experimentally the relation between group velocity and the average gap sizes. While our experimental apparatus is not able to resolve the nanometer-size gaps between individual particles, it is possible to estimate the effective, average gap size $\bar{\Delta}$ measuring variations in the length of the chains assembled in our setup. We construct loosely packed microscopic granular chains by assembling chains of particles without the use of precise micromanipulator compression, and measure the total distance $L$ between the 2nd and 13th particles. We calculate the average gap sizes in the different chains assembled as $\bar{\Delta} = L/(13-2) - 2R$ and estimate it to be between 250 and 500 nm, with a 30% accuracy limited by the optical resolution of the system. We strike each chain with a striker velocity of 0.01 m s and plot the distribution of measured group velocity for 45 different chains with the corresponding uncertainty. For each average gap, Eq. (2) provides an upper bound for the corresponding group velocity. We define the "allowed" (below the bound) and "forbidden" (above the bound) zones for the measured group velocities at varying average gaps and illustrate them in Fig. 4(c) as the orange and white areas, respectively. Due to the uncertainty in the experimental estimation of the striker velocity in Eq. (2), the boundary between the allowed and forbidden zones is not a simple curve but shown as an area with gradient color between orange and white, and width resulting from the uncertainty of $v_s$ (1 standard deviation). The experimental data is plotted in the graph with error bars, calculated with the uncertainty due to the optical inspection of the total length of the chain. It is evident that the measurements agree with the predicted zone.

The results provide experimental evidence of the suppression of group velocity in the presence of interparticle gaps.

In the presence of large interparticle gaps, the highly nonlinear solitary waves that characterize close-packed granular chains (described by the Nesterenko [2]) cease to exist. However, if the gaps are sufficiently small, the behavior of the system approximates the ideal, close-packed case. This occurs when $\frac{2R+\bar{\Delta}}{v_g^{(\mathrm{meas})}} \approx \frac{2R}{v_g^{(0)}} + \frac{\bar{\Delta}}{v_s} \approx \frac{2R}{v_g^{(0)}}$, or when $\frac{\bar{\Delta}}{v_s} \ll \frac{2R}{v_g^{(0)}}$, and

$$\bar{\Delta} \ll \frac{v_s}{v_g^{(0)}} 2R = 2.4\left(\frac{v_s}{c}\right)^{4/5} R. \tag{3}$$

Here, we use the relation between striker velocity and maximum particle velocity, $v_{\max} \approx 0.64 v_s$, which is obtained numerically for an uncompressed, close-packed, nondissipative granular chain with Hertzian interaction. This inequality shows that for stainless steel particles ($c = 4100\,\mathrm{m\,s}$) excited by a striker with velocity around 0.1 ms, the average interparticle gaps should be $\ll 0.05\%$ of the particle's radius in order to approximate the ideal chain response. As the size of the granular assemblies decreases, the required assembly precision increases. Additionally, this requirement increases even further if other types of imperfections are considered. For example, misalignment between microparticles leads to an offset (eccentricity) of the particle centers from the axis of the chain, which also affects the wave propagation. For two neighboring particles with slightly different radii ($R_{m+1}$ and $R_m$), the off-axis component of the contact force is $f_c e/2R$, where $e = |R_{m+1} - R_m|$. If this contribution exceeds the particle's confinements $f_{\mathrm{confine}}$, the chain fragments laterally. This suggests that in general, for the stabilities of granular assemblies, the condition $f_c e/2R \ll f_{\mathrm{confine}}$ needs to be satisfied during the excitation of the systems. In our analysis, we assume that the particle confinement is provided by the particle's own weight ($f_{\mathrm{confine}} = mg$, where $m$ is the mass of the particle and $g$ is the gravity of Earth) and neglect adhesive and frictional forces, for simplicity. To estimate the maximum contact force ($f_{c,\max}$) between the particles of a granular chain, we consider collisions between two free particles, assuming one is stationary and the other approaches with an initial velocity $v_s$. If the particle interaction is Hertzian, as shown in Eq. (1), the maximum interparticle force can then be derived as

$$f_{c,\max} = \frac{1}{6}\left(\frac{15}{2}\right)^{3/5}\left(\frac{E}{1-\nu^2}\right)^{2/5}\sqrt[5]{R}\,m^{3/5}{v_s}^{6/5}, \tag{4}$$

where $m$ is the mass, $R$ the radius, $E$ the elastic modulus, and $\nu$ the Poisson ratio of the particles.

In this case, to ensure no instabilities in a one-dimensional chain excited by a striker, this condition corresponds to an upper bound for eccentricity, $e$:

$$e \ll 5.3\frac{g}{{v_s}^{6/5}c^{4/5}}R^2. \tag{5}$$

Combining Eqs. (3) and (5), we obtain an expression, $\bar{\Delta}e^{2/3} \ll 7.3 g^{2/3} R^{7/3} c^{-4/3}$, to define an approximate bound for the imperfections without dependence on the striker velocity. Knowing fabrication limits, in terms of achievable average gap sizes $\bar{\Delta}$ and misalignment $e$, we can determine the minimal size of particles in a granular assembly that can support the formation and propagation of highly nonlinear solitary waves. In our experiment, we assume $\bar{\Delta} < 200$ nm (which is estimated to be the positioning precision of the particles in a chain) and $e < 1\ \mu$m (which corresponds to the nominal value of the particle radii variation for stainless steel 440c). These parameters lead to an estimate for the minimum particle radius $R = 670\ \mu$m required to support highly nonlinear solitary waves. This value is four times larger than the size of our particles, partially explaining the discrepancies observed between the experimental measurements of group velocities and the corresponding values calculated for an ideal granular chain (see Fig. 4).

## IV. CONCLUSIONS

In this work, we investigated the stress wave propagation in one-dimensional chains of microparticles. For the experiments, we constructed an apparatus employing laser-based excitation, noncontact high-speed microphotography and vibrometry, and a micromanipulator system. The setup allowed us to excite and study stress wave propagation in microgranular assemblies. We informed our experiments with discrete finite element simulations and modeled the system with Hertzian contact interaction. We obtained good agreement between experimental and numerical results for the decaying of the stress wave amplitude. However, a large deviation of the group velocity from theory was observed. We found that microscopic granular chains can support the propagation of highly nonlinear solitary waves under ideal conditions but are very sensitive to the presence of imperfections. We derived an analytical expression to relate the group velocity to the presence of interparticle gaps and support it with direct experimental evidence. In further analysis, we characterized the role of defects (gaps and misalignments) in the dynamic propagation of stress waves in a one-dimensional granular chain and defined analytical bounds for the scalability of a granular system with given assembly and fabricating precision. These findings can be used as guiding principles for implementation of engineering applications and scientific studies of microscopic granular systems.

## ACKNOWLEDGMENTS

The authors would like to acknowledge Prof. V. F. Nesterenko for fruitful discussions and Gladia Hotan for help in the experiments. This work has been supported by the MURI program, Project No. US ARO W911NF-09-1-0436, and made use of facilities supported by the Kavli Nanoscience Institute at Caltech.

[1] V. F. Nesterenko, J. Appl. Mech. Tech. Phys. **24**, 733 (1983).

[2] V. F. Nesterenko, *Dynamics of Heterogeneous Materials* (Springer, New York, 2001).

[3] N. Boechler, G. Theocharis, S. Job, P. G. Kevrekidis, M. A. Porter, and C. Daraio, Phys. Rev. Lett. **104**, 244302 (2010).
[4] S. Sen, J. Hong, J. Bang, E. Avalos, and R. Doney, Phys. Rep. **462**, 21 (2008).
[5] Y. Starosvetsky and A. F. Vakakis, Phys. Rev. E **82**, 026603 (2010).
[6] V. Tournat, V. Zaitsev, V. Gusev, V. Nazarov, P. Béquin, and B. Castagnède, Phys. Rev. Lett. **92**, 085502 (2004).
[7] C. Chong, F. Li, J. Yang, M. O. Williams, I. G. Kevrekidis, P. G. Kevrekidis, and C. Daraio, Phys. Rev. E **89**, 032924 (2014).
[8] D. Sun, C. Daraio, and S. Sen, Phys. Rev. E **83**, 066605 (2011).
[9] A. Leonard, L. Ponson, and C. Daraio, Extreme Mechanics Letters **1**, 23 (2014).
[10] A. Spadoni and C. Daraio, Proc. Natl. Acad. Sci. U.S.A. **107**, 7230 (2010).
[11] F. Li, C. Chong, J. Yang, P. G. Kevrekidis, and C. Daraio, Phys. Rev. E **90**, 053201 (2014).
[12] C. Daraio, V. F. Nesterenko, E. B. Herbold, and S. Jin, Phys. Rev. Lett. **96**, 058002 (2006).
[13] F. Fraternali, M. A. Porter, and C. Daraio, Mech. Adv. Mater. Struct. **17**, 1 (2009).
[14] R. Doney and S. Sen, Phys. Rev. Lett. **97**, 155502 (2006).
[15] J. Hong, Phys. Rev. Lett. **94**, 108001 (2005).
[16] N. Boechler, G. Theocharis, and C. Daraio, Nature Mater. **10**, 665 (2011).
[17] F. Li, P. Anzel, J. Yang, P. G. Kevrekidis, and C. Daraio, Nat. Commun. **5**, 5311 (2014).
[18] J. Xu, B. Zheng, and Y. Liu, Sci. Rep. **6**, 21052 (2016).
[19] C. Coste, E. Falcon, and S. Fauve, Phys. Rev. E **56**, 6104 (1997).
[20] C. Daraio, V. F. Nesterenko, E. B. Herbold, and S. Jin, Phys. Rev. E **72**, 016603 (2005).
[21] L. Feng, Z. Liuxian, T. Zhenhua, Y. Lingyu, and Y. Jinkyu, Smart Mater. Struct. **22**, 035016 (2013).
[22] C. Daraio, V. F. Nesterenko, E. B. Herbold, and S. Jin, Phys. Rev. E **73**, 026610 (2006).
[23] X. Ni, P. Rizzo, and C. Daraio, Phys. Rev. E **84**, 026601 (2011).
[24] J. R. Davis and A. S. M. I. H. Committee, *Stainless Steels* (ASM International, Materials Park, OH, 1994).